

CELL RESPONSE TO RGD DENSITY IN CROSSLINKED ARTIFICIAL
EXTRACELLULAR MATRIX PROTEIN FILMS

5.1 Abstract

This study examines the ability of crosslinked artificial extracellular matrix (aECM) protein films to alter cell adhesion, spreading, and migration. The aECM proteins described herein were originally designed for application in small-diameter grafts and are composed of elastin-like structural repeats and fibronectin cell-binding domains. aECM-RGD contains the RGD sequence from fibronectin, and aECM-RDG contains a scrambled cell-binding domain. Covalent attachment of poly(ethylene glycol) (PEG) to protein substrates reduced nonspecific cell adhesion to aECM-RDG-PEG but did not preclude sequence-specific adhesion of endothelial cells to aECM-RGD-PEG. Variation in ligand density was accomplished easily by mixing aECM-RGD-PEG and aECM-RDG-PEG. Increasing the density of RGD in the film resulted in more robust cell adhesion and spreading but did not have a significant effect on migration speeds. Cell-binding domain density in aECM proteins can thus be used to modulate cell adhesion and spreading and will serve as an important tool as these materials are further developed for use in tissue engineering.

5.2 Introduction

A central goal of tissue engineering is to design biomaterials that direct cellular interactions. In this way, seeding cells on a scaffold *ex vivo* could guide cells towards the desired phenotype to restore function. In other applications, replacement tissue could induce cells from the surrounding tissue to infiltrate and differentiate. One step towards achieving this goal has been to graft RGD and other cell adhesion sequences to polymers.¹ The bulk density of RGD peptides presented to cells has been shown to influence cell proliferation, adhesion, and migration properties.²⁻⁴ Nanoscale ligand clustering can also affect cell adhesion, motility, and differentiation.⁵⁻⁷ Furthermore, biochemical gradients have been shown to govern haptotaxis, cell distribution, and cell alignment.⁸⁻¹⁰ Use of a cell-adhesive ligand such as the RGD peptide therefore can serve as an important tool in controlling cell function.

Although peptide-grafted polymers have successfully manipulated cell responses, genetic engineering of proteins offers a facile method for developing materials that mimic the chemical and physical cues of the extracellular matrix (ECM). Because of the modular nature of recombinant DNA techniques, bioactive and structural domains from naturally occurring proteins can be incorporated easily into engineered proteins. Bacterial biosynthetic machinery then produces monodisperse samples in high yields. Many artificial protein-based materials thus have been developed for tissue engineering applications.¹¹⁻¹⁹

The family of artificial extracellular matrix (aECM) proteins described in this work was developed originally for use in small-diameter vascular grafts.²⁰⁻²⁷ Although synthetic materials such as poly(ethylene terephthalate) and expanded

poly(tetrafluoroethylene) have been successful in large-diameter grafts, their use in small-diameter grafts has been problematic.²⁸⁻³⁰ These grafts are thought to fail because of (i) the absence of a confluent endothelial layer and (ii) a compliance mismatch between the graft and surrounding tissue that leads to intimal hyperplasia and thrombosis. To address these issues, aECM proteins were designed with elastin-like repeats to confer elastomeric properties and cell-binding domains to promote endothelialization (Figure 5.1). By crosslinking lysine residues within the elastin-like domains, the modulus of a crosslinked, free-standing protein film can be tuned from 0.07 to 0.97 MPa.²² Furthermore, the design of these proteins allows for facile incorporation of different cell-binding domains, and previous work has studied the cell response to the RGD and CS5 cell-binding domains in adsorbed aECM proteins.^{20,23,25,27} aECM proteins thus allow for precise control over both biophysical and biochemical cues. In this study, we present a straightforward method for preparing crosslinked aECM films suitable for cell studies and examine the ability of protein films with differing RGD density to modulate cell adhesion, spreading, and migration.



Figure 5.1 Amino acid sequences of aECM proteins. aECM-RGD contains the RGD cell-binding domain. aECM-RDG is a negative control protein in which the cell-binding domain has been scrambled. Both proteins contain a T7 tag, a heptahistidine tag, an enterokinase cleavage site, and elastin-like domains with lysine residues that serve as crosslinking sites.

5.3 Materials and Methods

5.3.1 Protein Expression and Purification

aECM-RGD and aECM-RDG were expressed in *E. coli* and purified via temperature cycles as described previously.²⁵ The purity and molecular weight of the proteins were verified by SDS-PAGE gels, Western blots with an anti-T7 tag horseradish peroxidase-conjugated antibody (Novagen, San Diego, CA), amino acid analysis, and matrix-assisted laser desorption ionization-mass spectrometry (MALDI-MS).

5.3.2 Cell Culture

Human umbilical vein endothelial cells (HUVECs) were purchased from Cambrex BioSciences (Walkersville, MD) and maintained in a 37 °C, 5% CO₂ humidified environmental chamber. The cells were grown in endothelial growth medium-2 (EGM-2, 2% serum, Cambrex BioSciences); passages 2–7 were used in experiments. Near confluent HUVEC cultures were nonenzymatically detached by treatment with 0.61 mM EDTA.

5.3.3 Substrate Preparation

Aqueous aECM protein solutions (3.6 mg/mL) containing the bifunctional crosslinker bis(sulfosuccinimidyl) suberate (BS³, Pierce Biotechnology, Rockford, IL) were spread on a 12 mm base-cleaned glass coverslip. The molar ratio of activated ester to amine was 1:4. To slow the rate of crosslinking, protein solutions and coverslips were kept on ice. Coverslips were spin-coated at 4000 rpm for 45 s and stored overnight in a

humidified chamber at 4 °C. To covalently attach polyethylene glycol (PEG) to an aECM film, 50 µL of a 50 mM methoxy-PEG-succinimidyl propionate (mPEG-SPA, MW 5000, Nektar Therapeutics, San Carlos, CA) solution in water was placed on parafilm and the coverslips were placed protein-side down in the PEG solution. The coverslips were incubated for 2 h at room temperature, rinsed three times with water, sterilized with 95% ethanol for 1 h, and rinsed three times with water.

5.3.4 Substrate Characterization

To ensure uniformity, crosslinked protein films were examined via Western blots and fluorescence microscopy. Western blots were performed with an anti-T7 horseradish peroxidase-conjugated antibody. For fluorescence studies, films were blocked with 10% bovine serum albumin (BSA, fraction V, Sigma, St. Louis, MO) and incubated with an anti-T7 monoclonal antibody (Novagen) at a dilution of 1:2000 at room temperature overnight. After being rinsed three times with water, films were incubated with a Cy2-conjugated affinity-purified goat anti-mouse antibody (Chemicon, Temecula, CA) at a dilution of 1:10 for 1 h at room temperature. Coverslips were rinsed four times with water and examined on a Zeiss Axioplan II fluorescence microscope (Thornwood, NY) equipped with a monochrome Axiocam and AxioVision 3.1 software.

Crosslinked protein films were scratched with a razor blade to reveal the underlying glass substrate. Height was measured by imaging over the scratch with an AutoProbe M5 atomic force microscope (Park Scientific Instruments, Woodbury, NY) in constant-force contact mode, using pyramidal tips (0.58 N/m, Veeco DNP-S).

An M-probe surface spectrometer (Thermo VG Scientific, Waltham, MA) with monochromatic Al K α x-rays (1486.6 eV) was used for x-ray photoelectron spectroscopy (XPS). X-rays at an incident angle of 35° from the surface illuminated a 250 × 1000 μ m elliptical spot. A charge neutralizer was used because the samples were non-conductive. Ten detailed peak scans were collected with an instrument resolution of 1 eV and a step size of 0.1 eV. The ESCA 2000 analysis software v. 102.04 (Service Physics, Bend, OR) was used for peak integration. Three spots were analyzed on each substrate, and at least three substrates were examined for each condition.

Cell viability on crosslinked aECM proteins was measured by monitoring the cleavage of the tetrazolium salt WST-1 (Roche, Penzberg, Germany). After 24 h in serum-containing medium (EGM-2), there were no differences in viability between cells grown on aECM-RGD-PEG and those grown on fibronectin. Not surprisingly, the viability of cells grown on the negative control protein aECM-RDG-PEG was $43 \pm 10\%$ of the viability of cells grown on fibronectin. Three independent experiments were performed in triplicate.

5.3.5 *Cell Resistance to Detachment*

Experiments to measure cell resistance to normal detachment forces were adapted from a previously described method.²⁵ Briefly, each well of a black 24-well Visiplate (Perkin Elmer, Wellesley, MA) was blocked with 0.2% heat-inactivated BSA. Vacuum grease was applied to the undersides of dry coverslips to securely adhere them to the 24-well plate. After cells were fluorescently labeled with calcein acetoxymethyl ester (Molecular Probes, Carlsbad, CA), 1 mL of a cell suspension (2.67×10^5 cells/mL in

serum-free medium) was added to each well and incubated for 30 min on crosslinked protein films. The relative numbers of cells were measured by fluorescence (excitation at 485 nm and emission at 538 nm). Each well was filled with 1 mL of Percoll (21% w/w in PBS, Sigma), and the plates were centrifuged upright for 10 min at 100g. Because Percoll has a higher density (1.123 g/ml) than the cells (~1.07 g/ml), a buoyant force is exerted on the cells.^{6,31} Using Archimedes' theorem, the detachment force applied to each cell was estimated to be 26 pN. The liquid and non-adherent cells were removed, and the remaining cells were quantified by fluorescence. The fraction of cells retained in each well was calculated by dividing the fluorescence of the remaining cells by the fluorescence of the cells before centrifugation. A cell adhesion index (CAI) was calculated as the fraction of cells retained in a test well divided by the fraction of cells retained on fibronectin subjected to 1g (0.26 pN). Error bars represent standard deviations of three or more independent experiments performed in triplicate.

5.3.6 Cell Spreading

HUVECs in serum-free medium were seeded at a concentration of 4.8×10^4 cells per well in a 6-well plate. Cells on crosslinked aECM films were imaged at 15 min intervals by using a 10× phase contrast objective on a Nikon Eclipse TE300 inverted microscope. Pictures were manually scored for the number of spread (i.e., dark) versus non-spread (i.e., bright and refractive) cells. Three independent experiments were performed.

5.3.7 *Cell Migration*

Cells in EGM-2 were added to each well of a 6-well plate at concentrations of 1.6×10^4 to 6×10^4 cells per well. The cells were allowed to adhere for 2 h, after which they were imaged using a Nikon Eclipse TE300 inverted phase contrast microscope surrounded by a 37 °C incubation box. To maintain physiological pH, a humidified gas mixture of 5% CO₂, 20% O₂, and 75% N₂ was continuously bubbled through the 6-well plate. Teflon tape was used to seal the plate and a thin layer of mineral oil (embryo-tested, Sigma) was added to the top of the medium to prevent evaporation. Cells at various locations were recorded every 15 min for 24 h using a motorized stage and the MetaMorph Basic Imaging Software (Molecular Devices, Downingtown, PA).

The image sequences were imported into ImageJ 1.30v software (U.S. National Institutes of Health, Bethesda, MD) and saved as Quicktime files. Dynamic Image Analysis Software (DIAS) 3.2 (Solltech, Oakdale, IA) was used to analyze the Quicktimes movies. The images were thresholded to automatically trace cells. The outlines were then manually edited to erase incorrectly outlined areas and to adjust some tracings. Only cells whose paths were at least 8 h long were included in the analysis. At least three independent experiments were performed with a minimum of 80 cells tracked in total for each substrate.

5.4 Results and Discussion

5.4.1 Substrate Characterization

Protein films were prepared with a molar ratio of activated ester to amine of 1:4, which corresponds to 4.25 crosslinked amines per protein. A series of molar ratios were tested to ensure that crosslinking was sufficient to form a coherent film but would allow a degree of PEGylation that effectively reduced nonspecific cell interactions (see Figure 5.2, below). The height of the dry crosslinked aECM proteins was 8–10 nm as measured by atomic force microscopy (AFM). Western blotting and fluorescence imaging were used to verify film uniformity. When washed with water, ethanol, or 0.05% sodium dodecyl sulfate (SDS), the crosslinked protein films remained coherent. To further confirm that the proteins were crosslinked when prepared via this method, coverslips were spin-coated with protein solutions lacking the bifunctional BS³ crosslinker. When these coverslips were treated with water, fluorescence imaging indicated that the protein was not consistently distributed on the coverslip. Moreover, when these coverslips were exposed to a 0.05% SDS wash, little or no protein was detected on the coverslips. These results indicate that addition of the crosslinker is necessary for the uniformity and integrity of crosslinked aECM films.

5.4.2 PEGylation of Crosslinked aECM Films

To reduce nonspecific cell interactions with crosslinked aECM films, PEG was covalently attached to unreacted lysine residues in the aECM proteins. XPS was used to assess the fraction and number of PEGylated amines through comparison of the carbon to

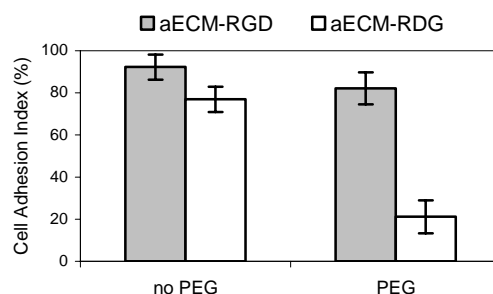


Figure 5.2 PEGylation reduces nonspecific cell adhesion on aECM films. HUVEC resistance to a detachment force of 26 pN is reported as percentages of HUVECs retained on aECM-RGD and aECM-RDG relative to fibronectin. Data represent three experiments, each performed in triplicate. Error bars represent one standard deviation.

nitrogen ratio of aECM films before and after PEGylation (see Table 5.1). After incubation with mPEG-SPA (MW 5000) for 2 h, XPS results indicated that ~1.8 PEG molecules were attached to each protein chain. There was no change to the number of PEG molecules linked to each protein when aECM films were treated with mPEG-SPA for longer times. When a PEG variant with no reactive ends (MW 4600) was used, the amount of PEG detected on the surface was equivalent to ~0.2 PEG molecules associated with each protein strand. Covalent attachment through lysine residues thus is necessary for effective PEGylation of aECM films.

Previous studies demonstrated that when these aECM proteins were adsorbed to a surface, cell adhesion was governed by interactions with the cell-binding domain.²⁵ In this work, we show that adhesion to crosslinked aECM proteins is also sequence-specific. HUVECs were incubated on the crosslinked substrates for 30 min and then subjected to a

26 pN normal detachment force for 10 min. On aECM proteins with or without PEG modification more cells remained adherent to aECM-RGD, containing the authentic cell-binding domain, than to aECM-RDG, the scrambled negative control protein (Figure 5.2). However, 3.9-fold more cells remained adherent to aECM-RGD than aECM-RDG when the films were modified with PEG (aECM-RGD-PEG and aECM-RDG-PEG, respectively) compared to 1.2-fold more cells when films were not modified with PEG. These results can be explained by the relatively high cell adhesion index (CAI) on aECM-RDG ($76.9 \pm 6.0\%$), which indicates that a large number of cells were nonspecifically attached to the surface. The CAI was reduced to $21.2 \pm 7.8\%$ when cells were seeded on aECM-RDG-PEG. All further cell studies were conducted with PEGylated crosslinked films.

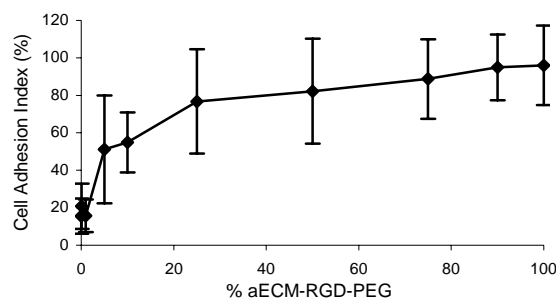


Figure 5.3 HUVEC resistance to detachment forces. By raising the concentration of aECM-RGD-PEG, the number of adherent cells can be increased. Crosslinked films were made by mixing aECM-RGD-PEG and aECM-RDG-PEG. Data represent three experiments, each performed in triplicate. Error bars represent one standard deviation.

5.4.3 HUVEC Resistance to Detachment Forces

Crosslinked films of varying aECM-RGD-PEG and aECM-RDG-PEG composition demonstrated that the number of adherent cells could be modulated by varying the number of available cell-binding domains. When films were composed of 0–1% aECM-RGD-PEG, the CAI was at background levels (16–21%). As the concentration of aECM-RGD-PEG was raised from 5 to 50%, the CAI increased from $51.1 \pm 28.8\%$ to $82.2 \pm 28.0\%$. At aECM-RGD-PEG concentrations greater than 75%, the CAI reached a plateau.

Based on the density of elastin (1.31 g/mL)³² and a polymer weight fraction of 0.56,³³ the concentration of cell-binding domains in the top 10 nm of hydrated aECM-RGD films is estimated as 3.8×10^5 cell-binding domains/ μm^2 (CBD/ μm^2). Previous results demonstrated that ligand densities ranging from 10^2 – 10^4 CBD/ μm^2 promoted cell adhesion,^{2,6,34} but few cells adhere to our substrate at 3.8×10^3 CBD/ μm^2 (corresponding to 1% aECM-RGD-PEG) and a minimum of 1.9×10^4 CBD/ μm^2 (corresponding to 5% aECM-RGD-PEG) is necessary for cells to adhere well to our proteins. Houseman and Mrksich have demonstrated that the microenvironment in which peptides are presented contributes strongly to cell adhesion; RGD peptides were attached to oligo(ethylene glycol) groups, and cell adhesion was found to be more sensitive to ligand density as the glycol oligomers were lengthened from three to six.³⁴ The PEG used in our work is much longer—it is estimated to have 100 glycol groups. Furthermore, the PEG is attached to the surface of the protein film and may impede cells from accessing the top 10 nm (as used in our calculation). The effective ligand density therefore may be lower than the calculated one. For these reasons we believe that, in order to elicit robust cell adhesion,

the calculated cell-binding domain density in our materials needs to be higher than previously reported values.

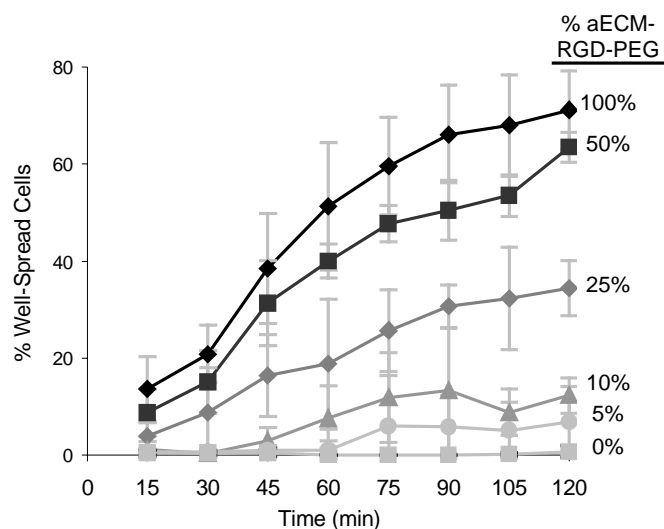


Figure 5.4 HUVEC spreading on crosslinked aECM films. Cell spreading kinetics can be modulated by varying aECM-RGD-PEG and aECM-RDG-PEG composition. Data represent three experiments. Error bars represent one standard deviation.

5.4.4 HUVEC Spreading on Crosslinked aECM Films

Crosslinked film composition also controlled cell spreading. Cells were monitored at 15 min intervals by phase contrast microscopy and categorized as dark and spread or bright and rounded. On films containing 50–100% aECM-RGD-PEG, half of the cells spread in the first 60–90 min (Figure 5.4). Reducing the aECM-RGD-PEG content to 25% resulted in only $34.4 \pm 10.6\%$ of the cells spreading at 2 h. When the aECM-RGD-PEG content was decreased even further to 5 and 10%, the percentages of spread cells at 2 h were $12.4 \pm 3.6\%$ and $6.9 \pm 7.2\%$, respectively. Less than 1% of the

cells spread on aECM films containing no authentic cell-binding sequences. The concentration of aECM-RGD-PEG can thus be used to manipulate the extent and rate of cell spreading.

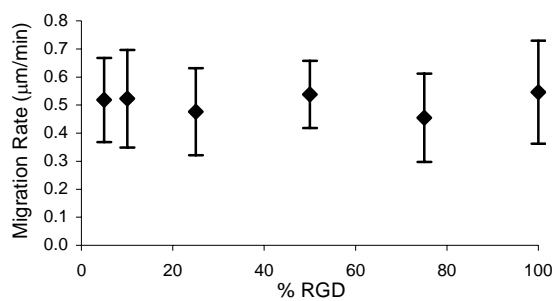


Figure 5.5 HUVEC migration on aECM substrates. Cell speed on aECM films does not correlate with aECM-RGD-PEG and aECM-RDG-PEG concentration. A minimum of 80 cells were tracked every 15 min for at least 8 h. Error bars represent one standard deviation.

5.4.5 HUVEC Migration Rates

A phase contrast microscope with a motorized stage and an environmental chamber was used to track cells every 15 min for a minimum of 8 h. Migration rate was calculated as the distance traveled divided by the duration of an interval. The measured HUVEC speeds ranged from 0.45–0.55 $\mu\text{m}/\text{min}$ but did not appear to correlate with concentration of cell-binding ligand. Published values for endothelial cells migrating on fibronectin or RGD peptides range from 0.25–0.67 $\mu\text{m}/\text{min}$;³⁵⁻³⁹ the migration speeds measured in this study fall within the upper half of reported values. Although previous studies have shown that cell migration rates can vary in a biphasic manner with respect to

cell-substratum adhesiveness,^{5,38,40} cells on our materials did not appear to exhibit this behavior. We believe this could be due to the low cell-substratum adhesiveness of our materials. In the study conducted by Maheshwari and coworkers, biphasic behavior was observed at mean detachment forces (i.e., the forces necessary to detach 50% of the plated cells) ranging from 250–1200 pN.⁵ Based on the adhesion data in Figure 5.3, the mean detachment force for cells on the 5% aECM-RGD-PEG film is 26 pN. Experimental results indicate that the mean detachment forces for films composed of 10–100% aECM-RGD-PEG are less than 195 pN (data not shown).

5.5 Conclusion

We have developed a method for making crosslinked aECM films suitable for cell studies. PEGylated protein substrates had low levels of nonspecific cell interactions but retained the ability to bind cells in a sequence-specific manner. We were able to modulate cell adhesion and spreading but not cell migration rates by varying the concentration of authentic cell-binding domains in the protein films. It has been demonstrated previously that endothelial cell mobility can be controlled through inclusion of other cell adhesion sequences such as the YIGSR peptide.^{36,39} Current work includes examining whether aECM proteins with ligands targeting different integrin receptors will be successful in modulating cell speed.

Cells respond not only to chemical cues such as peptide ligands but also to mechanical cues such as the stiffness of a material.⁴¹⁻⁴³ The mechanical properties of crosslinked aECM proteins can be manipulated through the molecular weights of the

proteins, the amount of crosslinker, and the protein weight fraction.^{21,22,24} Future studies will examine how cell responses can be modulated through both the chemical and mechanical properties of crosslinked aECM films.

5.6 Acknowledgments

We thank Paul Nowatzki for performing the AFM study, Elizabeth Jones and David Koos for advice on cell migration studies, Marissa Mock for helpful discussions on spin-coating protein films, Scott Fraser for help with fluorescence microscopy, and Caltech's Molecular Materials Research Center for help with the XPS. This work was supported by a Whitaker graduate fellowship to J.C.L.

5.7 Supporting Information

Supporting information includes 1) AFM height measurement of dry, crosslinked aECM-RGD and 2) XPS data on crosslinked aECM-RGD, aECM-RGD-PEG, and aECM-RGD + PEG MW 4600 with no reactive ends.

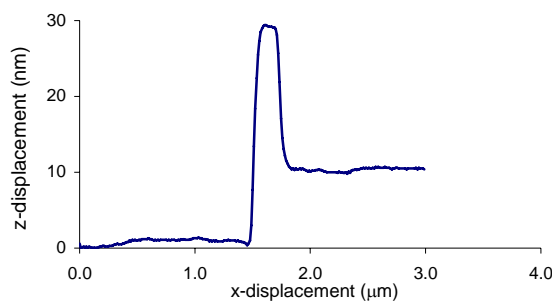


Figure 5.6 Representative AFM height measurement on crosslinked aECM-RGD. The film was scratched to reveal the underlying glass substrate. The dry height of the film was 8–10 nm.

| Substrates | Number | C/N Ratio | | | | PEGylation | |
|---------------------|--------|-----------|-------|-----------|-----------------|--------------------|-------------------------|
| | | Theor. | Avg. | Std. Dev. | Corrected Ratio | fraction of amines | # of amines per protein |
| aECM-RGD | 3 | 3.753 | 4.674 | 0.055 | | | |
| aECM-RGD-PEG | 7 | 10.573 | 5.653 | 0.563 | 0.979 | 0.11 | 1.8 |
| aECM-RGD + PEG 4600 | 4 | 3.753 | 4.756 | 0.114 | 0.082 | 0.01 | 0.2 |

Table 5.1 XPS data on crosslinked aECM-RGD, aECM-RGD-PEG, and aECM-RGD + PEG 4600 with no reactive ends. The numbers of substrates and the theoretical and measured carbon to nitrogen (C/N) ratios are shown. To account for the fact that the C/N ratio for aECM-RGD is higher than the theoretical value, a correction is done by subtracting the C/N ratio of aECM-RGD from the PEGylated versions. The fraction and number of PEGylated amines per protein are shown.

5.8 References

1. For review of RGD biomaterials: Hersel U, Dahmen C, Kessler H. RGD modified polymers: Biomaterials for stimulated cell adhesion and beyond. *Biomaterials* **2003**, *24*, 4385–4415.
2. Neff JA, Tresco PA, Caldwell KD. Surface modification for controlled studies of cell-ligand interactions. *Biomaterials* **1999**, *20*, 2377–2393.
3. Kantlehner M *et al.* Surface coating with cyclic RGD peptides stimulates osteoblast adhesion and proliferation as well as bone formation. *Chembiochem* **2000**, *1*, 107–114.
4. Rajagopalan P, Marganski WA, Brown XQ, Wong JY. Direct comparison of the spread area, contractility, and migration of balb/c 3T3 fibroblasts adhered to fibronectin- and RGD-modified substrata. *Biophys. J.* **2004**, *87*, 2818–2827.
5. Maheshwari G, Wells A, Griffith LG, Lauffenburger DA. Biophysical integration of effects of epidermal growth factor and fibronectin on fibroblast migration. *Biophys. J.* **1999**, *76*, 2814–2823.
6. Koo LY, Irvine DJ, Mayes AM, Lauffenburger DA, Griffith LG. Co-regulation of cell adhesion by nanoscale RGD organization and mechanical stimulus. *J. Cell Sci.* **2002**, *115*, 1423–1433.
7. Lee KY, Alsberg E, Hsiong S, Comisar W, Linderman J, Ziff R, Mooney D. Nanoscale adhesion ligand organization regulates osteoblast proliferation and differentiation. *Nano Lett.* **2004**, *4*, 1501–1506.
8. Brandley BK, Schnaar RL. Tumor cell haptotaxis on covalently immobilized linear and exponential gradients of a cell adhesion peptide. *Dev. Biol.* **1989**, *135*, 74–86.
9. Burdick JA, Khademhosseini A, Langer R. Fabrication of gradient hydrogels using a microfluidics/photopolymerization process. *Langmuir* **2004**, *20*, 5153–5156.

10. Kang CE, Gemeinhart EJ, Gemeinhart RA. Cellular alignment by grafted adhesion peptide surface density gradients. *J. Biomed. Mater. Res. Part A* **2004**, *71A*, 403–411.
11. Urry DW, Pattanaik A, Xu J, Woods TC, McPherson DT, Parker TM. Elastic protein-based polymers in soft tissue augmentation and generation. *J. Biomater. Sci.-Polym. Ed.* **1998**, *9*, 1015–1048.
12. Halstenberg S, Panitch A, Rizzi S, Hall H, Hubbell JA. Biologically engineered protein-graft-poly(ethylene glycol) hydrogels: A cell adhesive and plasmin-degradable biosynthetic material for tissue repair. *Biomacromolecules* **2002**, *3*, 710–723.
13. Nagarsekar A, Crissman J, Crissman M, Ferrari F, Cappello J, Ghandehari H. Genetic engineering of stimuli-sensitive silkelastin-like protein block copolymers. *Biomacromolecules* **2003**, *4*, 602–607.
14. Asakura T, Tanaka C, Yang M, Yao J, Kurokawa M. Production and characterization of a silk-like hybrid protein, based on the polyalanine region of *Samia cynthia ricini* silk fibroin and a cell adhesive region derived from fibronectin. *Biomaterials* **2004**, *25*, 617–624.
15. Girotti A, Reguera J, Rodriguez-Cabello JC, Arias FJ, Alonso M, Testera AM. Design and bioproduction of a recombinant multi(bio)functional elastin-like protein polymer containing cell adhesion sequences for tissue engineering purposes. *J. Mater. Sci.-Mater. Med.* **2004**, *15*, 479–484.
16. Nagapudi K, Brinkman WT, Thomas BS, Park JO, Srinivasarao M, Wright E, Conticello VP, Chaikof EL. Viscoelastic and mechanical behavior of recombinant protein elastomers. *Biomaterials* **2005**, *26*, 4695–4706.
17. Ogiwara K, Nagaoka M, Cho CS, Akaike T. Construction of a novel extracellular matrix using a new genetically engineered epidermal growth factor fused to IgG-Fc. *Biotechnol. Lett.* **2005**, *27*, 1633–1637.

18. Betre H, Ong SR, Guilak F, Chilkoti A, Fermor B, Setton LA. Chondrocytic differentiation of human adipose-derived adult stem cells in elastin-like polypeptide. *Biomaterials* **2006**, *27*, 91–99.
19. Foo CWP, Bini E, Huang J, Lee SY, Kaplan DL. Solution behavior of synthetic silk peptides and modified recombinant silk proteins. *Appl. Phys. A-Mater. Sci. Process.* **2006**, *82*, 193–203.
20. Panitch A, Yamaoka T, Fournier MJ, Mason TL, Tirrell DA. Design and biosynthesis of elastin-like artificial extracellular matrix proteins containing periodically spaced fibronectin CS5 domains. *Macromolecules* **1999**, *32*, 1701–1703.
21. Welsh ER, Tirrell DA. Engineering the extracellular matrix: A novel approach to polymeric biomaterials. I. Control of the physical properties of artificial protein matrices designed to support adhesion of vascular endothelial cells. *Biomacromolecules* **2000**, *1*, 23–30.
22. Di Zio K, Tirrell DA. Mechanical properties of artificial protein matrices engineered for control of cell and tissue behavior. *Macromolecules* **2003**, *36*, 1553–1558.
23. Heilshorn SC, Di Zio K, Welsh ER, Tirrell DA. Endothelial cell adhesion to the fibronectin CS5 domain in artificial extracellular matrix proteins. *Biomaterials* **2003**, *24*, 4245–4252.
24. Nowatzki PJ, Tirrell DA. Physical properties of artificial extracellular matrix protein films prepared by isocyanate crosslinking. *Biomaterials* **2004**, *25*, 1261–1267.
25. Liu JC, Heilshorn SC, Tirrell DA. Comparative cell response to artificial extracellular matrix proteins containing the RGD and CS5 cell-binding domains. *Biomacromolecules* **2004**, *5*, 497–504.
26. Heilshorn SC, Liu JC, Tirrell DA. Cell-binding domain context affects cell behavior on engineered proteins. *Biomacromolecules* **2005**, *6*, 318–323.

27. Richman GP, Tirrell DA, Asthagiri AR. Quantitatively distinct requirements for signaling-competent cell spreading on engineered versus natural adhesion ligands. *J. Control. Rel.* **2005**, *101*, 3–12.
28. Kannan RY, Salacinski HJ, Butler PE, Hamilton G, Seifalian AM. Current status of prosthetic bypass grafts: A review. *J. Biomed. Mater. Res. Part B* **2005**, *74B*, 570–581.
29. Vara DS, Salacinski HJ, Kannan RY, Bordenave L, Hamilton G, Seifalian AM. Cardiovascular tissue engineering: State of the art. *Pathol. Biol.* **2005**, *53*, 599–612.
30. Isenberg BC, Williams C, Tranquillo RT. Small-diameter artificial arteries engineered in vitro. *Circ. Res.* **2006**, *98*, 25–35.
31. Channavajjala LS, Eidsath A, Saxinger WC. A simple method for measurement of cell-substrate attachment forces: Application to HIV-1 Tat. *J. Cell Sci.* **1997**, *110*, 249–256.
32. Lillie MA, Gosline JM. Unusual swelling of elastin. *Biopolymers* **2002**, *64*, 115–126.
33. Nowatzki PJ, Franck C, Ravichandran G, Tirrell DA. Mechanically tunable thin films of photosensitive artificial proteins characterized by AFM nanoindentation. *In preparation* **2006**.
34. Houseman BT, Mrksich M. The microenvironment of immobilized Arg-Gly-Asp peptides is an important determinant of cell adhesion. *Biomaterials* **2001**, *22*, 943–955.
35. Chon JH, Netzel R, Rock BM, Chaikof EL. $\alpha_4\beta_1$ and $\alpha_5\beta_1$ control cell migration on fibronectin by differentially regulating cell speed and motile cell phenotype. *Ann. Biomed. Eng.* **1998**, *26*, 1091–1101.
36. Kouvroutoglou S, Dee KC, Bizios R, McIntire LV, Zygourakis K. Endothelial cell migration on surfaces modified with immobilized adhesive peptides. *Biomaterials* **2000**, *21*, 1725–1733.

37. Merzkirch C, Davies N, Zilla P. Engineering of vascular ingrowth matrices: Are protein domains an alternative to peptides? *Anat. Rec.* **2001**, *263*, 379–387.
38. Shiu YT, Li S, Marganski WA, Usami S, Schwartz MA, Wang YL, Dembo M, Chien S. Rho mediates the shear-enhancement of endothelial cell migration and traction force generation. *Biophys. J.* **2004**, *86*, 2558–2565.
39. Fittkau MH, Zilla P, Bezuidenhout D, Lutolf M, Human P, Hubbell JA, Davies N. The selective modulation of endothelial cell mobility on RGD peptide containing surfaces by YIGSR peptides. *Biomaterials* **2005**, *26*, 167–174.
40. Palecek SP, Loftus JC, Ginsberg MH, Lauffenburger DA, Horwitz AF. Integrin-ligand binding properties govern cell migration speed through cell-substratum adhesiveness. *Nature* **1997**, *385*, 537–540.
41. Discher DE, Janmey P, Wang YL. Tissue cells feel and respond to the stiffness of their substrate. *Science* **2005**, *310*, 1139–1143.
42. Pelham RJ, Wang YL. Cell locomotion and focal adhesions are regulated by substrate flexibility. *Proc. Natl. Acad. Sci. U. S. A.* **1997**, *94*, 13661–13665.
43. Engler A, Bacakova L, Newman C, Hategan A, Griffin M, Discher D. Substrate compliance versus ligand density in cell on gel responses. *Biophys. J.* **2004**, *86*, 617–628.